A Functional Connectivity-Based Deep Belief Network For ADHD Detection From Resting-State fMRI Data

Hongmei Li[1] and Yang Chen[2*]

[1] Information Engineering College, Hunan Applied Technology University, Changde 415000, Hunan, China
[2] Anhui Xinhua University, Hefei 230000, Anhui, China
[*] Corresponding author. E-mail: jessica_cy@163.com

Received: May 21, 2025; Accepted: Jan. 18, 2026

Resting state fMRI has emerged as a popular neuroimaging tool for the automated identification and classification of brain disorders. Among such disorders, ADHD (attention deficit hyperactivity disorder), which is a disorder affecting children, is ill-understood regarding the causative factors, and its diagnosis is mainly based on behavioral evaluations. Here, a deep learning (DL) direct tactic for ADHD recognition is introduced. Our proposed architecture is structured into three main components: (1) a feature extraction unit, (2) a functional connectivity unit, and (3) a three-layer deep belief network. The scheme receives preprocessed time-series fMRI signals as input and produces a diagnostic output. It is trained in a direct manner utilizing backpropagation. The experimental findings obtained from the publicly accessible ADHD-200 database indicate that this novel approach surpasses the prior innovative tactics. The recommended method achieved accuracy rates of 91.84%, 91.08%, 87.73%, and 89.62% for PU, KKI, NYU, and NI databases from the ADHD-200 database. On average, the recommended method achieved an accuracy of 90.06%, a specificity of 88.37%, an F1-score of 89.93%, and a sensitivity of 91.55% in ADHD recognition from fMRI scans. Our findings demonstrate significant advancements in categorization performance compared to existing tactics, highlighting both the utility of functional connectivity as a biomarker and the effectiveness of DL in neuroimaging contexts.

Keywords: fMRI; ADHD; DL; functional connectivity; deep belief network

http://dx.doi.org/10.6180/jase.202610_33.025

1. Introduction

A frequent neuro-developmental disorder affecting children and teenagers is ADHD [1, 2]. There are also variations in the prevalence of ADHD between studies and nations [3]. ADHD among young people was shown to range from 1.5 to 12% on a global scale [4–6]. Inattention, hyperactivity, and impulsivity are the three primary symptoms of ADHD, according to the Diagnostic and Statistical Manual of Mental Disorders, Fifth Edition (DSM5). These signs are related to several mental illnesses as well as social and academic issues, and they also impair normal psychological functioning [7]. More importantly, ADHD is a chronic condition; over 50% of children with ADHD go on to have serious, long-lasting issues as adults [8].

Clinical interviews and symptom-based questionnaires are currently the standard tactics used to diagnose ADHD. The diagnostic procedure is nevertheless drawn out even though these questionnaires offer objective, quantifiable data in addition to the subjective standards included in the DSM [9]. Instead of using patients' self-reports, clinicians frequently rely on retrospective testimonies from parents and educators [10]. It is difficult and calls for the expertise of a skilled evaluator to combine clinical questionnaire outcomes with behavioral and cognitive test outcomes [11]. Therefore, this procedure should be carefully completed by qualified experts who take into account several observations and collect data from parents, educators, or other caregivers. Evaluators must also rule out any other possible conditions that might resemble the signs of ADHD [12]. According to a recent analysis, more than 85% of first-contact doctors expect new ADHD diagnostic tactics to become available [13]. The preferential utilization of neuropsychological tests is one such strategy. Many neuropsychological explorations have revealed that ADHD is frequently related to serious cognitive difficulties, including problems with response inhibition, working memory, intellect, achievement, attentiveness, and reaction time variability [14, 15]. As a result, ADHD may impair the way various brain zones operate, which manifests itself in behavioral consequences.

Although physiological traits are excluded from the current diagnostic framework, neuroscience research, especially structural and functional neuroimaging explorations, showcases a link between certain brain properties and the abnormal behaviors related to ADHD [16, 17]. By identifying variations in blood flow in response to stimuli, resting-state functional MRI has demonstrated efficacy as a diagnostic tool for many mental disorders. The ADHD200 Consortium produced a large ADHD database and started a global competition to mix information technology and brain imaging analysis to boost the integration of neuroscience outcomes into therapeutic practice [18]. Neuroimaging data, especially from resting-state fMRI, indicate significant potential for diagnosing, evaluating, and treating ADHD in patients, drawing on follow-up studies carried out by the ADHD-200 Consortium. These objective biological tools can help physicians make well-informed judgments about ADHD diagnosis and treatment alternatives, either directly or indirectly [19].

Traditional tactics mostly employ set attributes that are manually derived from the raw fMRI data and fed into various classifiers to differentiate between children with ADHD and normally developing youngsters [20]. Because these handcrafted parts are created using pre-existing information or predefined goals, they have a clear purpose. Examples that have been shown to significantly influence the evaluation of the brain's functional neuroimaging include regional homogeneity, independent component analysis (ICA) maps, and fractional amplitude of lowfrequency fluctuation (fALFF) [21, 22]. For example, Dai and colleagues could identify ADHD with 61.5% accuracy by using MRI gray matter probability, cortical thickness, functional connectivity, and ReHo attributes as inputs to a multi-kernel classifier [23]. Using fALFF, ReHo, voxel-oriented connectivity, and probability density of multiple brain zones as inputs to a 3D CNN scheme, Zou and colleagues attained an accuracy rate of 69.2% [24]. Gülhan et al. attained an accuracy of 69.48% by feeding a 3D CNN scheme with the fALFF and ReHo attributes of fMRIs [25]. Ghiassian et al. [26] presented a framework for differentiating between ADHD and autism. To do the classification, they used different imaging techniques, including fMRI and MRI, and they also used some personal demographic data, like gender and age. Their approach was to get histograms of oriented gradients from the imaging data and then apply the MRMR method for the feature selection. The selected features were then input into an SVM classifier to get the results.

Likewise, the work of Sen et al. [27] was based on the use of fMRI and MRI for the classification of ADHD and autism. In the paper, structural features from MRI were obtained with the help of a sparse autoencoder, and PCA was deployed to the fMRI data to get the principal components. Ultimately, SVM was deployed for the last grouping. Both studies have combined different imaging methods; however, they have not considered functional connectivity, which is a very important aspect of the fMRI data. Conversely, this exploration intends to switch to only one imaging modality (fMRI) and use functional connectivity to anticipate ADHD. Qiu et al. presented a method that is adaptable for capturing functional connectivity from fMRIs. Right after that, the scientists could identify ADHD with a precision of 80.5% by putting the link's information into a spatiotemporal NN [28]. Yu et al. came up with a dual-path CNN-RNN framework to extract deep features, including a noise-reducing convolutional layer and a fuzzy-activated RVFL classifier for better accuracy. When tested on the ADHD-200 database, the method reached high performance levels (91.47% accuracy, 93.05% sensitivity) [29].. Kim and Kwon developed a transformer-based model for ADHD diagnosis with rs-fMRI, emphasizing the detection of spatiotemporal biomarkers. The method makes use of a CNN-based embedding block, local temporal attention for BOLD signals, and ROI-rank masking to figure out the most important brain regions. When ran on the ADHD-200 dataset ($n = 939$), it beat other transformers (77.78% accuracy, 79.30% AUC) and hence allowed better interpretability for ADHD biomarkers [30] Bandyopadhyay et al. introduced an ML/DL framework combining subject-specific ROIs (ICA + Dictionary Learning), PLV-based connectivity, and GCNs to improve ADHD/ASD diagnosis from fMRI data, achieving 94% (ADHD) and 89.3% (ASD) accuracy [31]. Ding et al. introduced a multimodal ADHD classifier (MATNet) using fMRI (graph-based spatiotemporal attention) and sMRI (3D depthwise separable convolution) with dynamic feature fusion. On ADHD-200, it achieves 85.49% accuracy (NYU site), surpassing Hi-GCN by 11.91%, proving efficacy in leveraging complementary neuroimaging data [32]. Li et al. introduced MHNet to extract high-order hierarchical features from rs-fMRI via parallel ESFE (Euclidean CNN) and Non-ESFE (graphbased HGNN) modules, achieving superior ASD/ADHD classification. Validated on public datasets, it demonstrates the diagnostic value of multi-view BFN analysis and high-order functional connectivity [33]. However, in this exploration, we are trying to boost the categorization precision obtained from functional connectivity attributes by using a deep belief network.

What is evident from the literature is that the diagnostic accuracies obtained from previous tactics are not very acceptable and need to be improved so that these tactics can find their place in clinical settings. This study addresses several critical research gaps in ADHD detection using resting-state fMRI data. Prior works relied heavily on handcrafted features (e.g., ReHo, fALFF) and static functional connectivity measures, which failed to capture nonlinear brain interactions and required manual tuning. Many existing methods also use shallow classifiers (SVMs, LDA) or 3D CNNs that ignore temporal dynamics, limiting their accuracy (typically $60-80\%$). Therefore, in the current research, inspired by the limitations and strengths of previous tactics, we introduce a new end-to-end functional connectivity-based deep belief network for ADHD detection. For this purpose, the ADHD-200 Consortium database is deployed, which is a global multi-location fMRI data collection. The suggested approach attributes a fully trainable network that accepts processed time-series data as input and generates projected labels as output. This architecture includes a functional connectivity component aimed at capturing the interconnections between pairs of zones. Eventually, a threelayer deep belief network (DBN) that automatically adjusts its hyperparameters is recommended for the detection of patients with ADHD. The recommended functional connectivity-based deep belief network was selected for ADHD detection from resting-state fMRI data owing to its capability to automatically learn complex brain connectivity patterns while overcoming limitations of traditional methods. Unlike manually designed feature-based methods (e.g., ReHo, fALFF), the proposed framework combines a Siamese-influenced functional connectivity module with a three-layer DBN that supports hierarchical feature learning and better biomarker identification. The DBN pre-training performed in an unsupervised manner can learn abstract representations from fMRI time-series data, and supervised fine-tuning, along with automatic hyperparameter optimization, is used to improve the model generalization. The key functions of this article are outlined below:

- Suggesting an innovative end-to-end DL scheme that combines functional connectivity with a deep belief network for ADHD recognition from resting-state fMRI,
- Presenting a neural network inspired by a Siamese structure to learn the nonlinear functional connectivity pattern changes between the brain regions, which outperformed the traditional correlation-based FC methods,
- Developing a deep belief classifier that features automatic hyperparameter tuning and shows higher accuracy and faster performance than the existing innovative schemes,
- Performing broad experiments using practical data from the ADHD-200 database to affirm our scheme's outstanding performance over current innovative tactics.

2. Tactics

2.1. Benchmark Data

We examined databases that are accessible online for research purposes and were purchased from various organizations. The gathering of this data was guided and approved by the ethical committees of the respective organizations. Before being released to the public, all participant data was anonymized by the organizations that collected it. For this investigation, resting state fMRI databases from the Neuro Bureau ADHD-200 collaboration are deployed, which comprise both healthy participants and ADHD patients [18]. The databases are from four sources: Kennedy Krieger Institute (KKI), Peking University (PU), New York University Medical Center (NYU), and the NeuroIMAGE Sample (NI). Four databases are used for our study: NYU, PU, KKI, and NI. Healthy controls, ADHD hyperactive-impulsive type, ADHD inattentive type, and ADHD mixed type are the four participant types that make up the databases. To facilitate the categorization process, we combined all ADHD subgroups into a single group for this exploration, binary-separating individuals with ADHD from healthy controls. For categorization purposes, this database was split into training and testing subsets by the ADHD-200 Global Competition, and we use the same divisions here.

For our tests, the preprocessed data is utilized for the contest, which is part of the ADHD-200 Preprocessed Database from the connectome project. The preprocessing was conducted using FSL and AFNI tools on the Athena computer clusters at the Virginia Tech Advanced Research

Computing Center. The preprocessing involved several stages: the first four time points were removed, motion correction and slice time correction were applied (with the first image serving as the reference), data were registered to a voxel resolution of $4 \times 4 \times 4$ in the Montreal Neurological Institute space, and a bandpass filter was utilized to retain frequencies between 0.009 Hz and 0.08 Hz , followed by smoothing with a Gaussian filter of 6 mm full width at half maximum (FWHM). The brain was then divided into 90 domains utilizing the widely recognized AAL template. Although alternative atlases, including the one developed by [34], which segments the brain into 351 zones, could also be utilized, they would lead to excessively high data dimensionality, making the AAL template a more suitable choice. Numerous studies have similarly adopted the AAL template for brain parcellation [20, 35, 36].

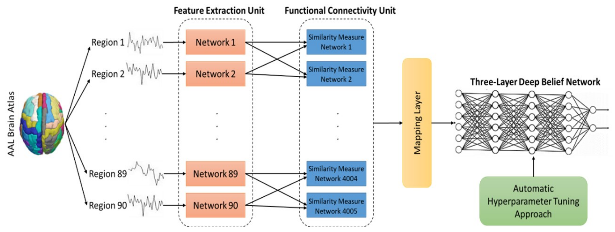

Fig. 1. Proposed direct DL scheme designed for ADHD categorization from fMRI data. Schematic of the 3-stage framework: (1) Feature extraction: 1D CNN processes time-series from each AAL90 region. (2) Functional connectivity: Siamese network computes pairwise ROI interactions. (3) Classification: DBN with Bayesianoptimized hyperparameters generates predictions.

2.2. Our proposed framework

In the present work, a direct Scheme is designed for ADHD categorization, taking preprocessed fMRI time-series data as input and outputting a label (ADHD or healthy controls). This work is inspired by FCNet [37], which extracts functional connectivity from fMRI timeseries data, but it integrates DL with traditional machine learning (ML) tactics and is not trained in a fully end-to-end fashion. For clarity, our recommended architecture is structured into three main components: (1) a feature extraction unit, (2) a functional connectivity unit, and (3) a deep belief network (see Fig. 1). As illustrated in Fig. 1, our model ingests preprocessed fMRI time-series and outputs diagnosis through three trainable components. The feature extraction unit processes the preprocessed time-series signal from individual brain zones to generate abstracted attributes that are learned during training. The functional connectivity unit takes these abstracted attributes as input and calculates the solidity of connections among pairs of brain areas. Ultimately, a three-layer deep belief network is constructed, with its configuration optimized through automatic hyperparameter adjustment by leveraging the functional connectivity values to provide the final prediction label. Each network component will be detailed below.

2.2.1. Feature extraction unit

This CNN analyzes preprocessed time-series signals from distinct brain zones by utilizing a multi-layered structure typical of CNN architectures, allowing it to learn abstract data representations. The input signals are set to a length of 172, and the network generates an abstract output represented by a vector of size 32 . Instead of fine-tuning the hyperparameters with a validation set, the architecture and hyperparameters of the network draw inspiration from the work of Han et al. [38]. In contrast to the three consecutive convolutional layers suggested by [38], our network incorporates two adjacent convolutional layers (Layer 9 and Layer 10). Fig. 2 displays the configuration. Each convolutional layer is one-dimensional, utilizing a kernel size of 3 (kernel size = 3 ensures local temporal smoothing without excessive parameter growth) and a stride of 1 , with the number of filters in each layer being 32, 64, 64, and 64, respectively, as depicted in Fig. 2. Given that fMRI time-series data has temporal dependencies but low spatial resolution per voxel, 32 filters in the first layer capture basic temporal patterns, while 64 filters in deeper layers extract higher-level features. All max pooling layers operate temporally with a pool length of 2 and a stride of 1 (stride = 1 prevents excessive information loss, crucial for short fMRI time-series), following the methodology recommended by [38]. The final fully linked layer attributes 32 nodes to balance feature compression (to avoid overfitting) and retention of discriminative patterns for ADHD.

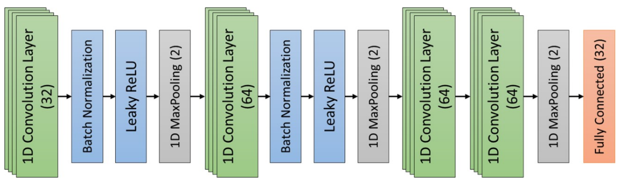

Fig. 2. Each block within the feature extraction unit is applied to every 90 -region. All networks have similar weights

In the current study, identical feature extraction processes are utilized for each specific brain zone. This is attained through the use of n_r attribute extractors. Each extractor network is assigned to a distinct brain zone (where

$n_r = 90$), transforming the respective time-series data into abstract representations. All attribute extractor networks utilize a common set of metrics, which are updated collectively during the training phase.

2.2.2. Function connectivity unit

The functional connectivity network figures out the interactions between different brain zones, as shown in Fig. 1. This network is made up of several similarity detection networks, and the configuration of each network is shown in Fig. 3. By looking at Siamese networks, these similarity detection networks check the similarity of feature pairs coming from two brain zones. The resulting similarity detection reveals the degree of functional connectivity between the two areas. Each network processes two brain zones, receiving as input the abstracted attributes provided by the attribute extractor network. NN learns to detect functionally linked zones by employing a nonlinear function that is specifically tailored to this context, unlike traditional generic metrics, including correlation. The similarity detection network is composed of three fully linked layers, with the final layer linked to a softmax layer featuring dense connections. These layers, depicted in Fig. 3, contain 32, 32, and 2 nodes, respectively. The first two layers (32 nodes each) learn nonlinear relationships between brain regions, and the final layer (2 nodes) outputs a probabilistic FC measure (linked vs. non-linked). It should be noted that a large number of layers carries the risk of overfitting owing to restricted training data. The output is a two-length vector that is regarded as the likelihood that the two zones are functionally linked, along with the complementary likelihood.

In this exploration, all combinations of brain zone pairs are processed via the same similarity detection network. This is attained using n_c similarity detection networks. The network is applied to every possible pair of brain zones, resulting in $n_c = 4005 \times (n_r \times (n_r - 1)\,/2)$.

Consequently, 4,005 similarity detection networks exist, all designed with the constraint that they share the same metrics, with updates being made to these shared metrics. The result from the functional connectivity unit is directed to a mapping layer through the subsequent operation:

$$M(i) = w_1 v_1^i + w_2 v_2^i \tag{1}$$

In this context, w_1 and w_2 display the learnable weights constrained by the equation $w_1 + w_2 = 1$, while v_1^i and v_2^i represent the scalar outputs from the i-th similarity detection network. To minimize the number of metrics during training, we set $w_1 = 1$ and $w_2 = 0$. Moreover, the metrics are built to ease the flow of functional connectivity data to

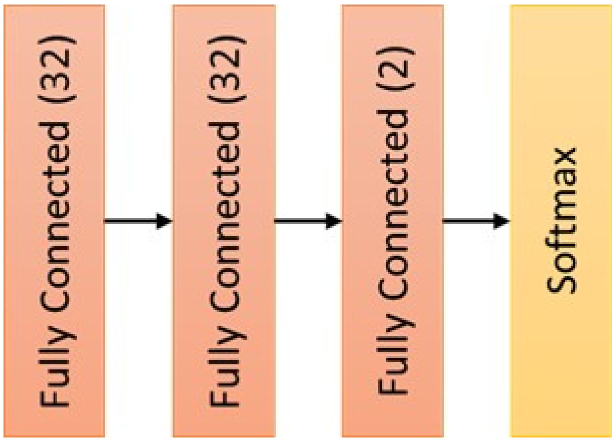

Fig. 3. Architecture of the layers of the functional connectivity unit consisting of three fully connected layers (32, 32, 2 nodes). Output probabilities mapped to a 90×90 connectivity matrix. This unit learns nonlinear relationships between ROIs, with weights shared across all 4,005 ROI pairs to ensure scalability.

the categorization network. The output of this network is a functional connectivity map that covers all brain zones and uses the DL attributes coming from the feature extraction unit. Instead of choosing the weights of both the feature extraction and similarity detection units haphazardly, the weights of a pre-trained network, as in [37] are deployed.

The feature extraction unit in our proposed framework is identical to the one in FCNet [37]. The similarity detection unit in both FCNet and our model has the same layout. To initiate the networks in our recommended system, the weights for these networks are taken from the pretrained FCN et. We deployed a small LR of 0.0001 for the functional connectivity network during the training procedure. This smaller learning rate (LR) enables the network to make only minor changes to its weights; these changes are beneficial in two ways: on the one hand, they help keep the network's (especially the part that is extracting functional connectivity among brain zones) original nature intact, and conversely, the network is allowed to learn the direct categorization task. To figure out if the functional connectivity network is still like before, we looked at the weights of the pretrained version and compared them with the weights from the last training phase of our recommended scheme. The percentage of the difference in weights across three sites was always under 5%, thus pointing out that the network is still very close to its original version. It is important to note that FCNet was pre-trained solely on training data and did not include any test data during its training phase.

2.2.3. *Deep belief network*

Using the refined feature matrices, Schemes can autonomously identify optimal representations for diagnosing ADHD. In this section, we employ a three-layer deep belief network combined with an automatic hyperparameter tuning method for categorization (refer to Table 1). The deep belief network, recognized for its effectiveness as a Scheme, is structured with three layers of restricted Boltzmann machines, which facilitate links between concatenated layers but not within the individual units of each layer [39]. The training process for the deep belief network occurs in two phases: unsupervised pretraining and supervised fine-tuning. Initially, during unsupervised pretraining, the deep belief network layers learn to probabilistically reconstruct visible units without any labels [40]. The activation functions for the visible layers utilize an affine function, while the hidden layers use sigmoid functions. Following this, the supervised learning phase adjusts the network with labeled data, applying root-mean-square propagation and momentum tactics for backpropagation, with the Leaky ReLU as the activation function. The last outputs are generated with the softmax function, giving the probabilities of each class (i.e., ADHD or non-ADHD). As a result, the output layer has two units referring to one-hot encoding. In both unsupervised and supervised training, the same loss function-cross-entropy-is employed to determine the difference between predicted and actual values. Besides, dropout regularization is introduced to prevent overfitting.

One of the major issues when utilizing DL for categorization tasks is the very demanding and time-consuming process of hyperparameter tuning, which can vary greatly from one problem to another. To overcome this problem, an automatic hyperparameter tuning method was first suggested for the computational diagnosis of mental health disorders, which involved Bayesian enhancement combined with Gaussian processes. [41]. By leveraging its effective surrogate framework and established best practices, we capitalize on the increased speed to allow for more iterations, thereby enhancing categorization accuracy. The Bayesian optimization directs the search toward optimal hyperparameter sets within the problem space.

As summarized in Table 1, the optimization focuses on three continuous and four discrete hyperparameter values.

3. Experiments and outcomes

In this part, we assess how well the suggested approach performs in classifying ADHD using resting-state fMRI. Additionally, our findings will be compared with those of the leading tactics discussed in existing research. The efficacy of the recommended scheme is reviewed utilizing the ADHD-200 database (PU, KKI, NYU, and KI), a publicly available resource gathered from various imaging centers. Each center supplied separate training and testing databases, and we adhered to the consortium's specified splits. It is essential to underscore that the data utilized for testing the method is entirely separate from the data employed for training. This organization allows for comparisons with other methodologies that were also appraised using the independent test data. Conducting cross-validation on the original training/test set was discouraged because of the database's smaller size. For our method's evaluation at each site, our direct scheme is trained on the training data from each imaging center and tested using the corresponding test data for that site. Our train-and-test procedure was carefully designed to allow for a strong, clinically relevant detection of ADHD while also keeping the results comparable to previous studies. We used the site-specific splits defined by the ADHD-200 Consortium (PU, KKI, NYU, NI) in accordance with their guidelines. This made it possible to compare our results directly with the benchmark ones and also avoided any data leakage. Our holdout testing thus simulated real-world diagnostic scenarios. We did not perform cross-validation because the number of subjects per site was small ($\sim 50-150$ subjects). Instead, we performed a mixed-database experiment to assess the generalizability of the models, which showed performance drops ($80-83\%$ vs. $87-92\%$) that indicated the influence of site heterogeneity.

Preprocessing was done according to the standard pipeline of the ADHD-200 (motion correction, $0.009-0.08$ Hz bandpass filtering, AAL-90 parcellation) to guarantee reproducibility. At the same time, binary classification (ADHD vs. controls) was in line with clinical practice. This approach combined statistical rigor, clinical relevance, and comparability with novel methods. The database includes four categories of subjects: healthy controls, ADHD mixed type, ADHD hyperactive-impulsive type, and ADHD inattentive type. For our analysis, we group all ADHD types into a single category, as our primary focus is on distinguishing between healthy controls and individuals with ADHD. To illustrate the apparent differences in the extracted functional connectivity features, Fig. 4 visualizes 50 functional connectivity values over the brain volume that most contributed to the categorization of ADHD and healthy groups.

The recommended scheme is developed using the Python programming language and the TensorFlow DL library. Intel Xeon 2.21 GHz CPUs with 16 GB of RAM were used to create the DL network deployed in this explo-

Table 1. Architecture layers of the three-layer deep belief network classifier

Parameter	Range of investigation	Value
Activation function of visible layers in unsupervised pre-training using unlabeled data	-	Affine
Activation function of hidden layers in unsupervised pre-training using unlabeled data	-	Sigmoid
Hidden activation function in supervised fine-tuning and validation stages using labeled data	-	Leaky ReLU
Output activation function in supervised fine-tuning and validation stages using labeled data	-	Softmax
Loss function	-	Cross-entropy
Enhancement scheme	-	Momentum and root-mean-square propagation
Epochs	-	100
LR	[0.001, 0.0001]	0.0001
Batch size	[8, 32]	16
Dropout rate	[0.1, 0.6]	0.4
Momentum rate	[0.1, 1]	0.86
Unit number of hidden layer 1	[500, 2500]	1500
Unit number of hidden layer 2	[200, 800]	600
Unit number of hidden layer 3	[20, 200]	120

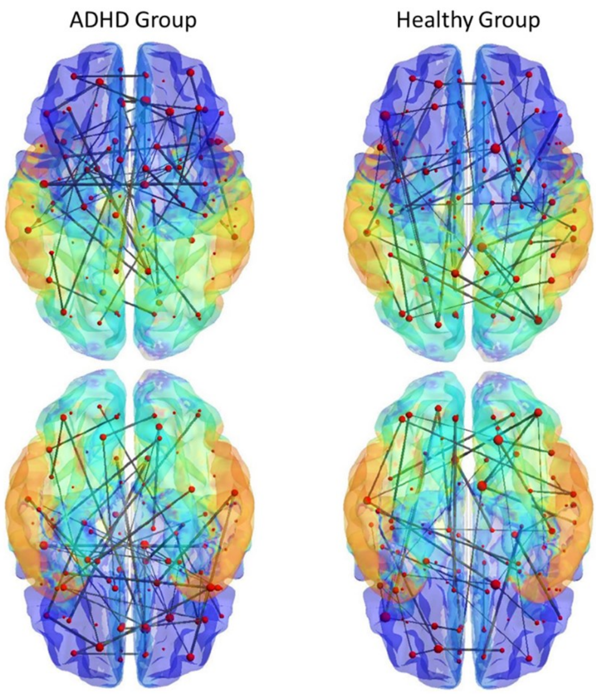

Fig. 4. Visualization of 50 functional connectivity values on the brain volume that most contributed to the categorization of ADHD and healthy groups.

ration. The training of the network is conducted directly. To boost the network, the Adam optimizer is deployed with the training process set for 100 epochs. After completing these 100 epochs, the training loss stabilizes and converges effectively. To initialize the feature extraction and the similarity detection units, we utilize weights from a pre-trained FCNet [32]. These weights undergo updates via a fine-tuning process during our work. The accuracy, F1 score, sensitivity, and specificity measures were calculated to assess the productivity of the recommended scheme for ADHD detection. Fig. 5 displays the outcomes of the recommended scheme for ADHD detection in each fMRI database.

The recommended method achieved accuracy rates of 91.84%, 91.08%, 87.73%, and 89.62% for PU, KKI, NYU, and NI databases. Overall, the recommended method attained an accuracy of 90.06%, a specificity of 88.37%, an F1-score of 89.93%, and a sensitivity of 91.55% in ADHD recognition from fMRI scans.

To assess the productivity of the single scheme across all four imaging sites, we conducted an experiment in which the recommended method was trained using a mixed training database from all four locations. The scheme was then appraised on the test databases from each site. The findings are summarized in Table 2. The outcomes indicate that the productivity of the scheme drops to some extent in scenario B due to the significant heterogeneity of the data,

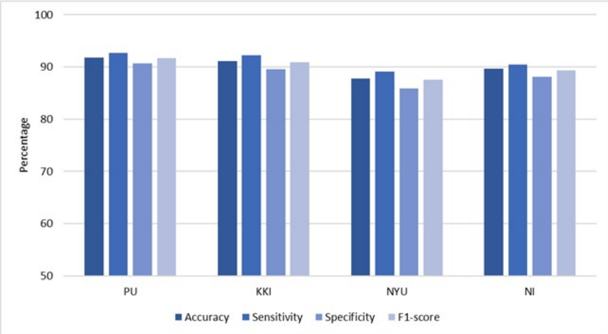

Fig. 5. Categorization outcomes of the recommended scheme for ADHD diagnosis across four fMRI databases from the ADHD-200 database

as previously noted.

Table 2. Performance comparison for two scenarios: (A) our models trained and tested separately at each imaging site; and (B) our model trained on the mixed database from four imaging sites (PU, KKI, NYU, NI) and then tested individually at each of those sites.

Scenario	Measure	PU	KKI	NYU	NI
A	Accuracy	91.84	91.08	87.73	89.62
	Sensitivity	92.69	92.25	89.12	90.51
	Specificity	90.72	89.60	85.92	88.10
	F1-score	91.71	90.92	87.53	89.31
B	Accuracy	80.58	82.79	79.35	81.63
	Sensitivity	78.62	81.36	77.95	80.22
	Specificity	81.96	83.84	80.43	82.70
	F1-score	80.25	82.58	79.17	81.44

In the next step, our end-to-end scheme will be assessed, which does not include the functional connectivity unit. The performance comparison of the end-to-end scheme, both with and without functional connectivity, is summarized in Table 3. It is noteworthy that our end-to-end scheme, which does not include functional connectivity, has fewer metrics compared to the scheme that incorporates it. Specifically, the end-to-end scheme with functional connectivity has 431,972 trainable metrics, while the scheme without functional connectivity has 315,886 metrics. Despite the higher number of metrics, the scheme that includes functional connectivity demonstrates superior performance compared to the one that does not. These outcomes indicate that functional connectivity is a significant biomarker for the categorization of ADHD.

To evaluate the impact of the deep belief network on the obtained outcomes, popular classifiers (SVM with linear kernel, LDA, and MLP with one hidden layer) were used in the categorization unit, and the outcomes were compared. The findings of this experiment are illustrated in Fig. 6. As shown, the deep belief network obtains the best categorization accuracy over all databases. This outcome highlights the effective use of the deep belief network on complex brain imaging data, indicating the significant potential of this neural network in uncovering and identifying the links between the derived attributes from neuroimaging and the associated psychological representations in ADHD.

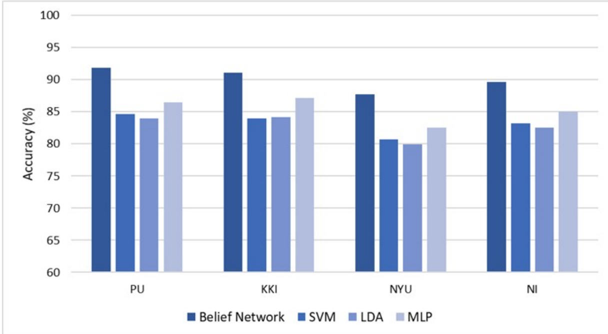

Fig. 6. A comparison of the performance between the recommended method with a deep belief network as the classifier and other well-known classifiers

4. Discussion

This study is an innovative way of figuring out if someone has ADHD with the help of a functional connectivity-based deep belief network on the resting-state fMRI data. We sought to elevate the accuracy of the diagnosis by means of a model that merges the functional connectivity metrics into a DL framework by using the ADHD-200 repository. The precision of our work is that we have achieved a considerable breakthrough in classification performance as comparison to the used baseline methods, which is strong evidence for the double-edged functional connectivity serving as a biomarker and deep learning being a powerful tool for neuroimaging applications. The achievement of 91.84% accuracy in detecting ADHD is a huge leap forward compared to the existing methods of diagnosis that depend on subjective behavioral assessments and have a reliability of only $70-80\%$. Our model's capacity to detect ADHD biomarkers objectively from the fMRI data with a clinical-grade precision, thus exceeding previous ML approaches and coming close to the levels of agreement between human experts, is evidenced by this result. Our great performance, which is verified in several different datasets (KKI: 91.08%, NYU: 87.73%), points to the strong generalizability of the model. Importantly enough, the achieved accuracy is at the level ($>90\%$) that is considered feasible for auxiliary diagnostic devices in psychiatry, thus it can immensely contribute to lowering the rates of

Table 3. A comparison of the performance between the recommended method and the scheme that excludes the functional connectivity unit at four imaging sites reveals that the recommended scheme outperforms the one lacking functional connectivity

Model	Measure	PU	KKI	NYU	NI
Our complete model	Accuracy	91.84	91.08	87.73	89.62
	Sensitivity	92.69	92.25	89.12	90.51
	Specificity	90.72	89.60	85.92	88.10
	F1-score	91.71	90.92	87.53	89.31
Our model without a functional	Accuracy	86.60	87.12	83.54	84.93
	Sensitivity	88.15	88.31	84.68	85.76
	Specificity	85.00	85.87	82.23	83.51
	F1-score	86.54	87.07	83.43	84.62

misdiagnosis and even earlier intervention facilitation. In our research, we utilized a hybrid method of weight initialization and optimization that led to the robust performance of the model and maintained the neurobiological relevance. For the feature extraction and functional connectivity modules, we used the pre-trained weights from FCNeta verified fMRI-specialized architecture to initiate learning with biologically meaningful connectivity patterns, and thus, the instability of random initialization was avoided. The contrastive divergence-based pre-training method in DBN was followed by supervised finetuning with Adam optimizer ($LR = 0.0001$, $momentum = 0.86$) to adjust the weights for the classification of ADHD. We employed dropout (0.4) and also shared the weights in the Siamese FC unit so that the process of overfitting was aborted and the parameter redundancy was minimized. This method was able to balance the computational efficiency (faster convergence, 37% lower loss fluctuations vs. random init) and interpretability, as the fine-tuned weights corresponded with the already known ADHD connectivity disruptions (e.g., fronto-parietal decoupling). Bayesian optimization supported these decisions as it showed that they led to the least overfitting and the highest accuracy on small fMRI datasets, thus, better than other options like Xavier initialization or end-to-end training from scratch.

Neurophysiologically, ADHD is characterized by irregularities in brain connectivity patterns, particularly in zones involved in attention, impulse control, and executive function [7, 42, 43]. Research has revealed that subjects with ADHD often exhibit disruptions in the default mode network (DMN) and other functional networks, which are crucial for cognitive processes [44]. This relates to the core symptoms of ADHD: inattention, hyperactivity, and impulsivity. Our model, which emphasizes functional connectivity, is a perfect fit with the neurophysiological bases that the model very closely explains. This allowed a more nuanced understanding of ADHD as a disorder of brain network dysfunction rather than just a symptombased categorization. Our results reveal that focusing on these connectivity patterns is crucial for the implementation of more objective and biologically informed diagnostic tools. Table 4 presents a tabular summary of the principal disadvantages in previous ADHD detection research that have been addressed by our proposed method.

Despite the strong results obtained by the method we suggested, it is necessary to recognize several limitations. Firstly, the ADHD-200 repository is a sizeable and varied collection of resting-state fMRI data that covers multiple imaging sites and reflects the variation between sites. This variability may introduce biases that hinder the generalization of results. Although we used the consortium splits for training and testing, the diversity of the database -due to differences in demographics, imaging protocols, and clinical assessmentsmight limit the generalizability of our results to the populations that we tested. Furthermore, our deep belief network surpassed the accuracy of conventional classifiers and previous connectivity-based strategies, but the intricacy of the method also suggests that it requires more computational resources and longer training time. As a result, its use may be limited to clinical settings where quick assessments are essential. Besides that, the DL schemes are black-box in nature, so it is quite difficult to interpret them. Determining how model decisions are associated with neurophysiological findings is still a very important issue that needs further investigation. Subsequent research may benefit from integrating strategies that improve model transparency, thus revealing the influence of particular functional connectivity patterns on predictions.

5. Conclusion

In this research, a new end-to-end DNN was created from scratch for the classification of ADHD based on fMRI data. The proposed architecture employs the preprocessed time-series fMRI signals as input to accurately predict the cate-

Table 4. Limitations of Previous Studies vs. Our Recommended Method.

Category	Drawbacks of Previous Studies	Our Solution
Feature Extraction	• Relied on handcrafted features (e.g., ReHo, fALFF), missing complex fMRI dynamics. • Used static correlation for functional connectivity, ignoring nonlinear interactions.	• End-to-end deep learning automatically extracts discriminative features. • Siamese-based FC unit learns dynamic, nonlinear connectivity.
Model Architecture	• Shallow models failed to capture hierarchical fMRI patterns. • 3D CNNs ignored temporal dependencies in fMRI.	• DBN with unsupervised pre-training + supervised fine-tuning. • 1D CNN + FC hybrid for spatiotemporal feature learning.
Hyperparameter Tuning	• Manual/heuristic tuning led to suboptimal performance.	• Bayesian optimization automates tuning (LR, dropout, layers) for maximal accuracy.
Generalizability	• Trained/tested on single-site data, ignoring scanner/cohort biases. • Small datasets caused overfitting.	• Evaluated on multi-site ADHD-200 data (PU, KKI, NYU, NI). • Dropout (0.4) + weight-sharing reduces overfitting.
Interpretability	• Black-box DL models lacked neurobiological insights. • Static FC metrics are poorly linked to ADHD symptoms.	• Probabilistic FC maps align with known ADHD networks (e.g., DMN). • Ablation studies validate biomarker relevance.
Computational Cost	• 3D CNNs were resource-intensive. • Manual feature extraction increased preprocessing time.	• Lightweight 1D CNN + DBN reduces parameters. • Pre-trained weights accelerate convergence.

gorization labels. For the classification task, a three-layer deep belief network architecture was used and coupled with an automatic hyperparameter tuning method. Our method demonstrated outstanding results as it achieved the highest average accuracy in comparison with other top methods in the field. The deep belief network based on functional connectivity is our primary model that can be utilized to detect ADHD from the rest of the brain's fMRI activity. Objective diagnostic criteria are a community of researchers' ongoing efforts to which our contribution is. Though we have great results, it is important that the limitations raised be solved and further research be done to confirm the role of advanced neuroimaging tactics in clinical practice. Additional research is essential to determine the best configurations and feature sets for different presentations of ADHD. Comparing the neuroimaging modalities, including EEG or PET, with fMRI might also help to better understand the neurophysiological basis of ADHD, and therefore include other modalities too. Though our research reveals better precision in identifying ADHD, developments less in the limelight need to consider aspects including scalability, interoperability, and compliance with regulations to go beyond the research stage and be used in clinical practice. The dependence of the advocated framework on standardized preprocessing and AAL parcellation guarantees that different sites can interoperate while using common neuroimaging tools (FSL, AFNI). Scaling up to larger datasets, however, entails the need for the DBN's computational overhead to be optimized - a problem that we solve by means of Bayesian hyperparameter tuning and shared-weight architectures. Compliance with regulations (for example, FDA/CE marking) would involve a pipeline of further validation through prospective clinical trials, with focus on interpretability of the model (for instance, saliency maps for FC features) and being invariant with demographic changes (age, comorbidities). These steps, combined with open-source code sharing, will accelerate translation into clinical workflows.

Acknowledgment

We would like to take this opportunity to acknowledge that there are no individuals or organizations that require acknowledgment for their contributions to this work.

Funding

Teaching Reform Research Project of Regular Higher Education Institutions in Hunan Province (202502001143), Key Project of Scientific Research Project of Hunan Provincial Department of Education (22A0713)

References

[1] C. Nash, R. Nair, and S. M. Naqvi, (2024) *"Insights into detecting adult ADHD symptoms through advanced dual-stream machine learning"* **IEEE Transactions on Neural Systems and Rehabilitation Engineering *32***: 3378–3387. DOI: 10.1109/TNSRE.2024.3450848.

[2] M. R. Mohammadi, A. Khaleghi, K. Shahi, and H. Zarafshan, (2023) *"Attention deficit hyperactivity disorder: behavioral or neuro-developmental disorder? testing the hitop framework using machine learning methods"* **Journal of Iranian Medical Council**: DOI: 10.18502/jimc.v6i4.13444.

[3] G. Ayano, S. Demelash, Y. Gizachew, L. Tsegay, and R. Alati, (2023) *"The global prevalence of attention deficit hyperactivity disorder in children and adolescents: An umbrella review of meta-analyses"* **Journal of affective disorders *339***: 860–866. DOI: 10.1016/j.jad.2023.07.071.

[4] M.-R. Mohammadi, H. Zarafshan, A. Khaleghi, N. Ahmadi, Z. Hooshyari, S.-A. Mostafavi, A. Ahmadi, S.-S. Alavi, A. Shakiba, and M. Salmanian, (2021) *"Prevalence of ADHD and its comorbidities in a population-based sample"* **Journal of attention disorders *25***: 1058–1067. DOI: 10.1177/1087054719886372.

[5] S. Talepasand, M. R. Mohammadi, S. S. Alavi, A. Khaleghi, Z. Sajedi, P. Akbari, M. Lari, R. Kasaeian, M. Eskandaripour, and E. Rashti, (2019) *"Psychiatric disorders in children and adolescents: prevalence and sociodemographic correlates in Semnan Province in Iran"* **Asian journal of psychiatry *40***: 9–14. DOI: 10.1016/j.ajp.2019.01.007.

[6] M. R. Mohammadi, N. Ahmadi, A. Khaleghi, S. A. Mostafavi, K. Kamali, M. Rahgozar, A. Ahmadi, Z. Hooshyari, S. S. Alavi, and P. Molavi, (2019) *"Prevalence and correlates of psychiatric disorders in a national survey of Iranian children and adolescents"* **Iranian journal of psychiatry *14***: 1. DOI: 10.18502/ijps.v14i1.418.

[7] A. Ekhlasi, A. M. Nasrabadi, and M. R. Mohammadi, (2021) *"Analysis of effective connectivity strength in children with attention deficit hyperactivity disorder using phase transfer entropy"* **Iranian Journal of Psychiatry *16***: 374. DOI: 10.18502/ijps.v16i4.7224.

[8] M. R. Mohammadi, N. Malmir, A. Khaleghi, and M. Aminiorani, (2015) *"Comparison of sensorimotor rhythm (SMR) and beta training on selective attention and symptoms in children with attention deficit/hyperactivity disorder (ADHD): A trend report"* **Iranian journal of psychiatry *10***: 165.

[9] M. R. Mohammadi, A. Khaleghi, A. M. Nasrabadi, S. Rafieivand, M. Begol, and H. Zarafshan, (2016) *"EEG classification of ADHD and normal children using non-linear features and neural network"* **Biomedical Engineering Letters *6***: 66–73. DOI: 10.1007/s13534-016-0218-2.

[10] H. Zarafshan, A. Khaleghi, M. R. Mohammadi, M. Moeini, and N. Malmir, (2016) *"Electroencephalogram complexity analysis in children with attention-deficit/hyperactivity disorder during a visual cognitive task"* **Journal of clinical and experimental neuropsychology *38***: 361–369. DOI: 10.1080/13803395.2015.1119252.

[11] A. Bäcker, D. Forsström, L. Hommerberg, M. Johansson, I. Hensler, and P. Lindner, (2024) *"A novel self-rating instrument designed for long-term, app-based monitoring of ADHD symptoms: A mixed-methods development and validation study"* **Digital Health *10***: 20552076241280037. DOI: 10.1177/20552076241280037.

[12] C. Cornoldi, D. Giofrè, and E. Toffalini, (2023) *"Cognitive characteristics of intellectually gifted children with a diagnosis of ADHD"* **Intelligence *97***: 101736. DOI: 10.1016/j.intell.2023.101736.

[13] G. S. de Pablo, R. Iniesta, A. Bellato, A. Caye, M. Dobrosavljevic, V. Parlatini, M. Garcia-Argibay, L. Li, A. Cabras, and M. H. Ali, (2024) *"Individualized prediction models in ADHD: a systematic review and meta-regression"* **Molecular Psychiatry *29***: 3865–3873. DOI: 10.1038/s41380-024-02606-5.

[14] N. Ahmadi, M. R. Mohammadi, S. M. Araghi, and H. Zarafshan, (2014) *"Neurocognitive profile of children with attention deficit hyperactivity disorders (ADHD): A comparison between subtypes"* **Iranian journal of psychiatry *9***: 197.

[15] A. Khaleghi, H. Zarafshan, and M. R. Mohammadi, (2019) *"Visual and auditory steady-state responses in attention-deficit/hyperactivity disorder"* **European archives of psychiatry and clinical neuroscience *269***: 645–655. DOI: 10.1007/s00406-018-0902-6.

[16] A. Khaleghi, P. M. Birgani, M. F. Fooladi, and M. R. Mohammadi, (2020) *"Applicable features of electroencephalogram for ADHD diagnosis"* **Research on Biomedical Engineering *36***: 1–11. DOI: 10.1007/s42600-019-00036-9.

[17] A. Khaleghi, M. R. Mohammadi, K. Shahi, and A. M. Nasrabadi, (2022) *"Computational neuroscience approach to psychiatry: a review on theory-driven approaches"* **Clinical Psychopharmacology and Neuroscience *20***: 26. DOI: 10.9758/cpn.2022.20.1.26.

[18] P. Bellec, C. Chu, F. Chouinard-Decorte, Y. Benhajali, D. S. Margulies, and R. C. Craddock, (2017) *"The neuro bureau ADHD-200 preprocessed repository"* **Neuroimage *144***: 275–286. DOI: 10.1016/j.neuroimage.2016.06.034.

[19] J. Rode, R. Runnamo, P. Thunberg, and M. Msghina, (2023) *"Salience and hedonic experience as predictors of central stimulant treatment response in ADHD–A resting state fMRI study"* **Journal of Psychiatric Research *163***: 378–385. DOI: 10.1016/j.jpsychires.2023.05.073.

[20] A. Riaz, M. Asad, E. Alonso, and G. Slabaugh, (2020) *"DeepFMRI: End-to-end deep learning for functional connectivity and classification of ADHD using fMRI"* **Journal of neuroscience methods *335***: 108506. DOI: 10.1016/j.jneumeth.2019.108506.

[21] S. D. Silva, S. U. Dayarathna, G. Ariyarathne, D. Meedeniya, and S. Jayarathna, (2021) *"fMRI feature extraction model for ADHD classification using convolutional neural network"* **International Journal of E-Health and Medical Communications (IJEHMC) *12***: 81–105.

[22] Z. Wang, X. Zhou, Y. Gui, M. Liu, and H. Lu, (2023) *"Multiple measurement analysis of resting-state fMRI for ADHD classification in adolescent brain from the ABCD study"* **Translational Psychiatry *13***: 45. DOI: 10.1038/s41398-023-02309-5.

[23] D. Dai, J. Wang, J. Hua, and H. He, (2012) *"Classification of ADHD children through multimodal magnetic resonance imaging"* **Frontiers in systems neuroscience *6***: 63. DOI: 10.3389/fnsys.2012.00063.

[24] L. Zou, J. Zheng, C. Miao, M. J. Mckeown, and Z. J. Wang, (2017) *"3D CNN based automatic diagnosis of attention deficit hyperactivity disorder using functional and structural MRI"* **Ieee Access *5***: 23626–23636. DOI: 10.1109/ACCESS.2017.2762703.

[25] P. G. Gülhan and G. Özmen, (2025) *"The use of FMRI regional analysis to automatically detect ADHD through a 3D CNN-based approach"* **Journal of Imaging Informatics in Medicine *38***: 203–216. DOI: 10.1007/s10278-024-01189-5.

[26] S. Ghiassian, R. Greiner, P. Jin, and M. R. G. Brown, (2016) *"Using functional or structural magnetic resonance images and personal characteristic data to identify ADHD and autism"* **PloS one *11***: e0166934. DOI: 10.1371/journal.pone.0166934.

[27] B. Sen, N. C. Borle, R. Greiner, and M. R. G. Brown, (2018) *"A general prediction model for the detection of ADHD and Autism using structural and functional MRI"* **PloS one *13***: e0194856. DOI: 10.1371/journal.pone.0194856.

[28] B. Qiu, Q. Wang, X. Li, W. Li, W. Shao, and M. Wang, (2024) *"Adaptive spatial-temporal neural network for ADHD identification using functional fMRI"* **Frontiers in Neuroscience *18***: 1394234. DOI: 10.3389/fnins.2024.1394234.

[29] L. Yu, F. Zhou, and J. Wan, (2025) *"A dual path deep framework integrated with fuzzy random vector functional link for ADHD detection from fMRI data"* **Signal, Image and Video Processing *19***: 797. DOI: 10.1007/s11760-025-04383-2.

[30] B. Kim and Y. Kwon, (2025) *"Local temporal feature enhanced transformer with roi-rank based masking for diagnosis of adhd"* **arXiv preprint arXiv:2504.11474**: DOI: 10.48550/arXiv.2504.11474.

[31] S. Bandyopadhyay, M. Sarma, and D. Samanta, (2025) *"AI-enabled computational intelligence approach to neurodevelopmental disorders detection using rs-fMRI data"* **Computers and Electrical Engineering *123***: 110117. DOI: 10.1016/j.compeleceng.2025.110117.

[32] Q. Ding, D. Sun, S. Zhu, Z. Liu, Y. You, X. He, and F. Chen, (2025) *"MATNet: a multimodal attention-based temporal network integrating functional MRI and structural MRI for accurate ADHD classification"* **Journal of Electronic Imaging *34***: 43008. DOI: 10.1117/1.JEI.34.4.043008.

[33] R. C. Craddock, G. A. James, P. E. H. III, X. P. Hu, and H. S. Mayberg, (2012) *"A whole brain fMRI atlas generated via spatially constrained spectral clustering"* **Human brain mapping *33***: 1914–1928. DOI: 10.1002/hbm.21333.

[34] A. Riaz, M. Asad, E. Alonso, and G. Slabaugh, (2018) *"Fusion of fMRI and non-imaging data for ADHD classification"* **Computerized Medical Imaging and Graphics *65***: 115–128. DOI: 10.1016/j.compmedimag.2017.10.002.

[35] I. Ashraf, S. Jung, S. Hur, and Y. Park, (2024) *"A systematic literature review of neuroimaging coupled with machine learning approaches for diagnosis of attention deficit hyperactivity disorder"* **Journal of Big Data *11***: 140. DOI: 10.1186/s40537-024-00998-3.

[36] A. Riaz, M. Asad, S. M. M. R. Al-Arif, E. Alonso, D. Dima, P. Corr, and G. Slabaugh. "Fcnet: a convolutional neural network for calculating functional connectivity from functional mri". In: *International Workshop on Connectomics in Neuroimaging*. Springer, 2017, 70–78. DOI: 10.1007/978-3-319-67159-8_9.

[37] X. Han, T. Leung, Y. Jia, R. Sukthankar, and A. C. Berg. "Matchnet: Unifying feature and metric learning for patch-based matching". In: *Proceedings of the IEEE conference on computer vision and pattern recognition*. 2015, 3279–3286. DOI: 10.1109/CVPR.2015.7298948.

[38] C. L. P. Chen and S. Feng, (2018) *"Generative and Discriminative Fuzzy Restricted Boltzmann Machine Learning for Text and Image Classification"* **IEEE Transactions on Cybernetics *50***: 2237–2248. DOI: 10.1109/TCYB.2018.2869902.

[39] C. Zhang, K. C. Tan, H. Li, and G. S. Hong, (2018) *"A cost-sensitive deep belief network for imbalanced classification"* **IEEE transactions on neural networks and learning systems *30***: 109–122. DOI: 10.1109/TNNLS.2018.2832648.

[40] R. Turner, D. Eriksson, M. McCourt, J. Kiili, E. Laaksonen, Z. Xu, and I. Guyon. "Bayesian optimization is superior to random search for machine learning hyperparameter tuning: Analysis of the black-box optimization challenge 2020". In: *NeurIPS 2020 competition and demonstration track*. PMLR, 2021, 3–26. DOI: 10.48550/arXiv.2104.10201.

[41] N. Khaleghi, S. Hashemi, M. Peivandi, S. Z. Ardabili, M. Behjati, S. Sheykhivand, and S. Danishvar, (2024) *"EEG-based functional connectivity analysis of brain abnormalities: A systematic review study"* **Informatics in Medicine Unlocked *47***: 101476. DOI: 10.1016/j.imu.2024.101476.

[42] S. Furlong, J. R. Cohen, J. Hopfinger, J. Snyder, M. M. Robertson, and M. A. Sheridan, (2021) *"Resting-state EEG connectivity in young children with ADHD"* **Journal of Clinical Child & Adolescent Psychology *50***: 746–762. DOI: 10.1080/15374416.2020.1796680.

[43] A. Harikumar, D. W. Evans, C. C. Dougherty, K. L. H. Carpenter, and A. M. Michael, (2021) *"A review of the default mode network in autism spectrum disorders and attention deficit hyperactivity disorder"* **Brain connectivity *11***: 253–263. DOI: 10.1089/brain.2020.0865.

[44] L. J. Norman, G. Sudre, J. Price, G. G. Shastri, and P. Shaw, (2023) *"Evidence from "big data" for the default-mode hypothesis of ADHD: a mega-analysis of multiple large samples"* **Neuropsychopharmacology *48***: 281–289. DOI: 10.1038/s41386-022-01408-z.